Available online at www.sciencedirect.com

ScienceDirect

Energy Procedia 76 (2015) 565 – 572

Energy Procedia

European Geosciences Union General Assembly 2015, EGU

Division Energy, Resources & the Environment, ERE

Subsurface porous media hydrogen storage - scenario development and simulation

Wolf Tilmann Pfeiffer*, Sebastian Bauer

Institute of Geosciences, University of Kiel, 24105 Kiel, Germany

Abstract

Subsurface porous media hydrogen storage could be a viable option to mitigate shortages in energy supply from renewable sources. In this work, a scenario for such a storage is developed and the operation is simulated using a numerical model. A hypothetical storage site is developed, based on an actual geological structure. The results of the simulations show that the storage can supply about 20 % of the average demand in electrical energy of the state of Schleswig-Holstein, Germany, for a week-long period.

Peer-review under responsibility of the GFZ German Research Centre for Geosciences

Keywords: hydrogen; energy storage; subsurface porous media storage; numerical simulations

1. Introduction

Electric energy production from renewable sources is governed by the availability of the individual energy source, i.e. wind or solar radiation. Therefore, natural fluctuations in availability can lead to shortages in energy production if the share of renewable sources in the total energy production is significant. One possibility to mitigate these shortages is to employ an energy storage scheme. While motives have changed over time, the idea of using hydrogen energy storage is not entirely new and has already been adressed by several authors (e.g. [1–4]). Geological storage is a possible option to store large quantities of hydrogen and therefore large amounts of energy over long timescales [1,2,5–7]. Hydrogen can be stored using either salt caverns or porous formations like saline aquifers or depleted gas fields. While hydrogen has already been stored successfully in salt caverns for industrial use in Texas, USA and Tesside, UK [8], experiences with subsurface porous media hydrogen storage are relatively scarce. So far only hydrogen-rich town gas has been stored in an aquifer near Baynes, France [1,2]. In this paper we therefore define a possible usage scenario and investigate the system behaviour of a hypothetical subsurface porous media hydrogen storage site in northern Germany using numerical scenario simulations.

* Corresponding author. Tel.: +49-431-880-4805; fax: +49-431-880-7606.
E-mail address: wolf_tilmann.pfeiffer@gpi.uni-kiel.de

Peer-review under responsibility of the GFZ German Research Centre for Geosciences
doi:10.1016/j.egypro.2015.07.872

2. Scenario definition

In the case of hydrogen energy storage the scenario definition consists of the quantification of the volume of hydrogen which has to be stored in order to meet target energy demand as well as the selection and parametrization of a suited storage site.

2.1. Storage demand

The storage demand is a function of the duration of the energy shortage period and the required delivery rate of energy. Numerical simulations of energy production in a 100 % renewables scenario based on actual meterological data show continuous shortages in energy production of up to 14 days in one month [4]. During these gaps only little to no energy at all is available from the primary sources. Since other short- and medium term energy storage would most likely be employed as well, the period of demand was assumed to be one week. The most basic assumption to asses the required delivery rate of energy is to cover the average consumption of electrical energy in the local region. While this approach does not take into account daily fluctuations in demand and supply, it serves as a worst case scenario as it assumes no energy production from primary sources at all. In 2011 a total of 42.82 mio. GJ of electrical energy was used in the state of Schleswig-Holstein, Germany [9]. Therefore, the amount of energy which has to be supplied to ensure deliverability for one week was estimated to be around 0.82 mio. GJ. The efficiency of the hydrogen re-electrification process used has to be taken into account when quantifying the required hydrogen gas volume. The re-electrification can be done using fuel cells [10–12] or gas turbines [4,13,14]. The precise efficiency value depends on the individual type of fuel cell or turbine used. Since the range given for both pathways is relative similar, an efficiency of 60 % was assumed for the re-electrification process. In combination with the volumetric energy density of hydrogen at standard conditions of 0.0106 GJ/m^3 [1], the required storage volume to compensate for a weeklong outage of the complete energy production from primary sources results to be 129 mio. sm^3 (volume at surface conditions) of hydrogen.

2.2. Storage site

Underground storage of natural gas, which has been performed successfully over several decades at various sites, can be used as an analogue for subsurface porous media hydrogen storage [1,2]. The potential storage site should therefore meet demands comparable to those set for the storage of natural gas. Among those are a sufficient reservoir volume, competent upper and lower sealing formations preventing the gas from migration as well as a sufficient permeability to ensure well deliverability [15]. Due to the risk of fingering of the gas phase in the storage formation, a steeply dipping structure is favourable [16]. The depth of the storage formation is also important for well deliverability as it affects the pressure drop within the well. This pressure drop is directly proportional to the length of the well [1,17], thus reducing the well length by selecting moderately deep storage formations is beneficial.

The geological setting of the hypothetical storage simulated in this work is based on an anticlinal structure in Schleswig-Holstein. The structure was formed by halokinesis of the Zechstein salt group which started in the Triassic [18]. During the evolution of the structure several northwest-southeast oriented faults formed which pose a possible threat to the integrity of the caprock [19]. The Rhaetian deposits of the upper Triassic were selected to be used as the storage formation since they meet most of the criteria stated and have proven to be a reservoir formation suited for natural gas exploration in Germany [20]. The Rhaetian of Northern Germany consists of several sandstones layers with intermediate shale layers [19,21,22]. The depositional environment changes from a non-marine system in the eastern part through a paralic system to a marine setting in the west [22]. Caused by early Cimmerian uplift, the Rhaetian deposits at the storage site are partially eroded [22,23]. Thus, the storage resembles a capped dome structure (Fig. 1a). The geological model used in this work is based on a regional structural model developed by Hese [19]. The depth of the Rhaetian deposits at the storage site ranges from around 400 m at the top of the structure to more than 3000 m at the flanks (Fig. 1b). Due to the difference in depth, the shallower eastern flank of the structure was chosen to accommodate the storage. Thus, only the eastern half of the anticline was included in the simulation in order to reduce the required computational effort. Based on facies descriptions by Gaupp [21] and Hese [19] the Rhaetian deposits at the storage site were further subdivided into the Upper Rhaetian, the upper shale of the Middle Rhaetian, the main sandstone of the Middle Rhaetian, the lower shale of the Middle Rhaetian and the Lower Rhaethian. It has

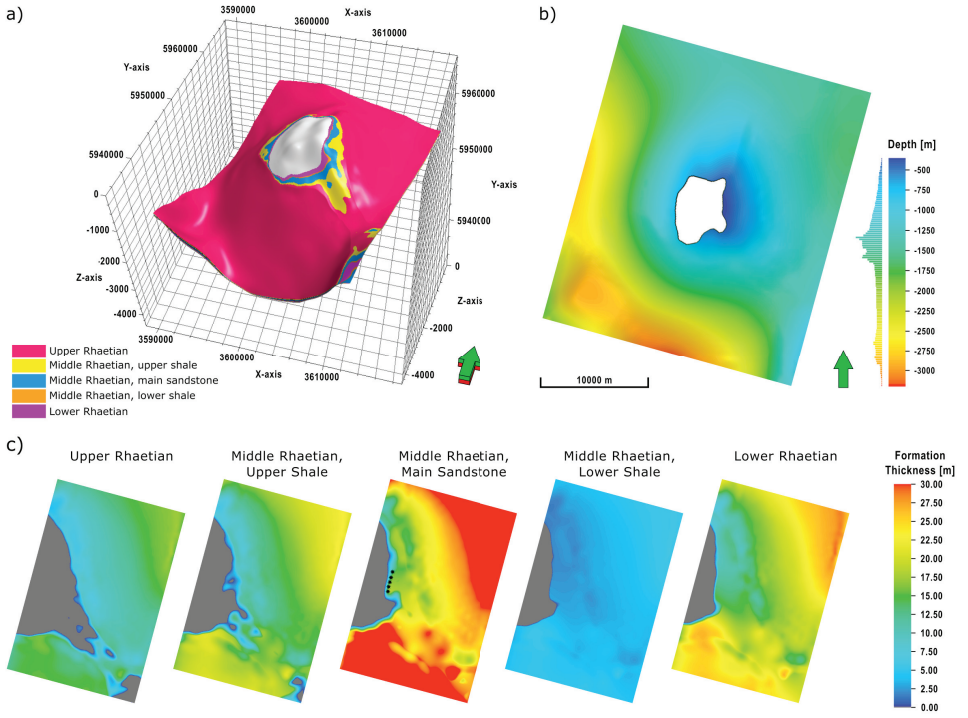

Fig. 1. (a) Structure of the Rhaetian deposits including the sub-formations; (b) depth of the Rhaetian base; (c) thickness of the Rhaetian sub-formations in the model. The position of the wells in the storage formation are indicated as black dots.

to be mentioned that, despite their names, all sub-formations consist of various sandstone as well as shale layers. The thickness of the individual sub-formations varies from less than 5 m for the lower shale of the Middle Rhaetian to more than 30 m for the main sandstone of the Middle Rhaetian (Fig. 1c). The target reservoir formation is the main sandstone of the Middle Rhaetian.

Hydraulic parameters porosity (θ) and permeability ($\mathbf{k}$) were assigned based on on-site data [19] and off-site data of the same formation [21]. Unfortunately, neither on- nor off-site data on capillary pressures and relative phase permeabilities was available. Capillary pressure data was calculated using a standard Brooks & Corey function [24] while the relative permeability data was calculated using a Corey-type equation [25]. The necessary values for the residual water saturations ($S_{r,water}$), displacement pressures (p_d) as well as maximum relative permeabilities of the gas phase (k_{rg0}) and the pore distribution index (λ) were assigned based on values found in literature for rocks with comparable porositities and permeabilities (e.g. [26–29]). In order to reduce model complexity a homogeneous distribution of the hydraulic parameters was assumed within each sub-formation of Rhaetian (Tab. 1).

Table 1. Hydraulic parameters used in the simulation.

Formation	$\mathbf{k}$ [mD]	θ [-]	p_d [bar]	$S_{r,water}$ [-]	k_{rg0} [-]	λ [-]
Upper Rhaetian	2.25	0.14	0.5	0.4	0.3	2.5
Middle Rhaetian, upper shale	27.5	0.16	0.5	0.4	0.3	2.5
Middle Rhaetian, main sandstone	572.2	0.33	0.1	0.3	0.9	2.5
Middle Rhaetian, lower shale	2.1	0.13	0.5	0.4	0.3	2.5
Lower Rhaetian	41.8	0.14	0.2	0.4	0.5	2.5

3. Scenario simulation

The simulated hydrogen storage operation is conducted using five wells that are located near the top of the anticlinal structure at a depth between 460 - 490 m. The well placement is based on the local thickness as well as on the geometry of the reservoir formation, the main sandstone of the Middle Rhaetian. To maximize the theoretical deliverability of the storage, all wells are completed over the whole formation thickness resulting in completion lengths of around 12 to 13 m.

Prior to the initial filling of the reservoir with the cushion gas, a hydrostatic pressure distribution is assumed throughout the reservoir. Furthermore, open model boundaries are assumed. Compressibility of the fluid phases and the solid phase are assumed while diffusion is not considered in the simulation. The fluid densities and viscosities are calculated using a generalized formulation of the Peng-Robinson equation of state [30]. The model is spatially discretized into 50 × 50 m cells with a varying cell thickness ranging from 0.2 m to over 5 m depending on the formation thickness. The simulation is carried out using the multiphase-multicomponent reservoir simulator Eclipse E300 [30].

The simulated storage operation is split into three main phases. At first the cushion gas is injected into the storage formation with a target rate of 56625 sm^3/day/well for 710 days. Nitrogen is used as cushion gas as it is relatively inert to chemical reactions and is considered cheap due to its great abundance in the geosphere [31,32]. In the second phase of the storage operation the composition of the injected gas is switched to the working gas, i.e. hydrogen, while the injection rate is simultaneously increased to 155000 sm^3/day/well. The duration of the second storage phase is 210 days. In the third phase four storage cycles are simulated, each consisting of an extraction of gas from the storage over a period of one week followed by an injection of hydrogen for 50 days and a subsequent shut-in period of 30 days. The target rates for extraction and injection during the third phase are set to 1000000 sm^3/day/well and 150000 sm^3/day/well respectively. The achievable gas flow rates, however, are constrained by upper and lower bottom hole pressure limits set to 65 and 30 bar respectively. Under optimal conditions the dimensioning of the storage should be therefore be sufficient to yield about 27 % of the energy demand defined in chapter 2.1.

4. Results

Within the first 10 days of the initial filling with N_2, the bottom hole pressure in all wells reaches the upper limit of 65 bar. The bottom hole pressures do not decrease during the first two stages of the storage operation, the injection of N_2 and the initial filling with H_2, as the gas is injected continuously. In order to comply with the pressure limits, the applied injection rates are subsequently reduced automatically (Fig. 2). As a result, less gas than projected is injected into the storage formation. The individual performance of the wells varies strongly within the first and the

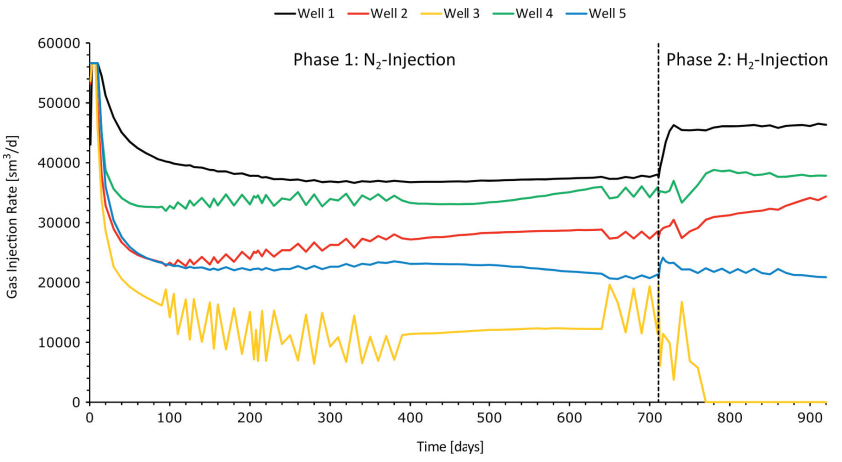

Fig. 2. Achieved gas injection rates for all wells in storage phase 1 and 2.

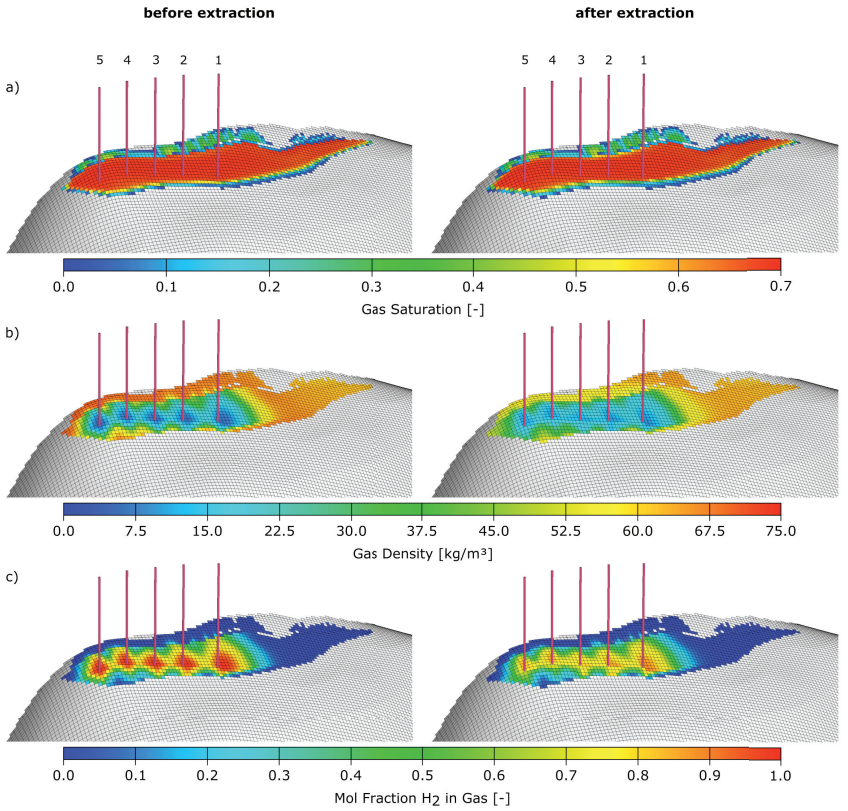

Fig. 3. (a) Gas saturation; (b) gas density; (c) H_2 in gas before and after the fourth storage cycle in storage phase 3. Viewing direction is towards the west.

second storage phases with none of the wells being able to reach the target rate. The northernmost well 1 is the best performing well with an injection rate of 37000 sm^3/day in the first storage phase and 46000 sm^3/day in the second storage phase. Well 4 is following closely behind with around 35000 and 47000 sm^3/day for phase one and two respectively. While wells 2 and 5 start off with comparable rates they diverge during storage phase one with well 2 reaching around 28000 sm^3/day and well 5 slowly declining to about 20000 sm^3/day. During the second storage phase the performance of well 5 continuous to be on the same level while the injection rate of well 2 increases further to about 37000 sm^3/day. The center well 3 is the worst performing well of the storage. During the first phase well rates of less than 14000 sm^3/day are achieved. About 60 days into the second storage phase the well is shut completely as it can not flow at the limiting bottom hole pressure. On average an injection rate of 28775 sm^3/day/well and 27771 sm^3/day/well is reached in the first and second storage phase respectively.

Both gas components that are injected into the reservoir have a significantly lower density than the initially present formation water. As a result the injected gas accumulates in the top of the structure (Fig. 3a). Due to the geometry of the reservoir formation, a part of the gas migrates away from the wells towards the northern model boundary. The thickness of the storage formation decreases directly north of the wells, thus the amount of migrated gas is smaller than it seems. During the simulation period, the majority of the gas remains in the storage formation while a small volume of gas migrates into the underlying formations, mainly the sandstones of the Lower Rhaetian. The comparison of the gas phase distribution before and after the extraction shows only very minor differences. This is in part due to the small volume of extracted gas relative to the total gas in place and the compression and expansion of the gas phase which dampens the water movement. The latter is also visible in the change in gas density over the course of the production period (Fig. 3b). As the individual density of the gas components at reservoir conditions differs by slightly less than one order of magnitude, the gas density also roughly corresponds to the spatial distribution of the gas

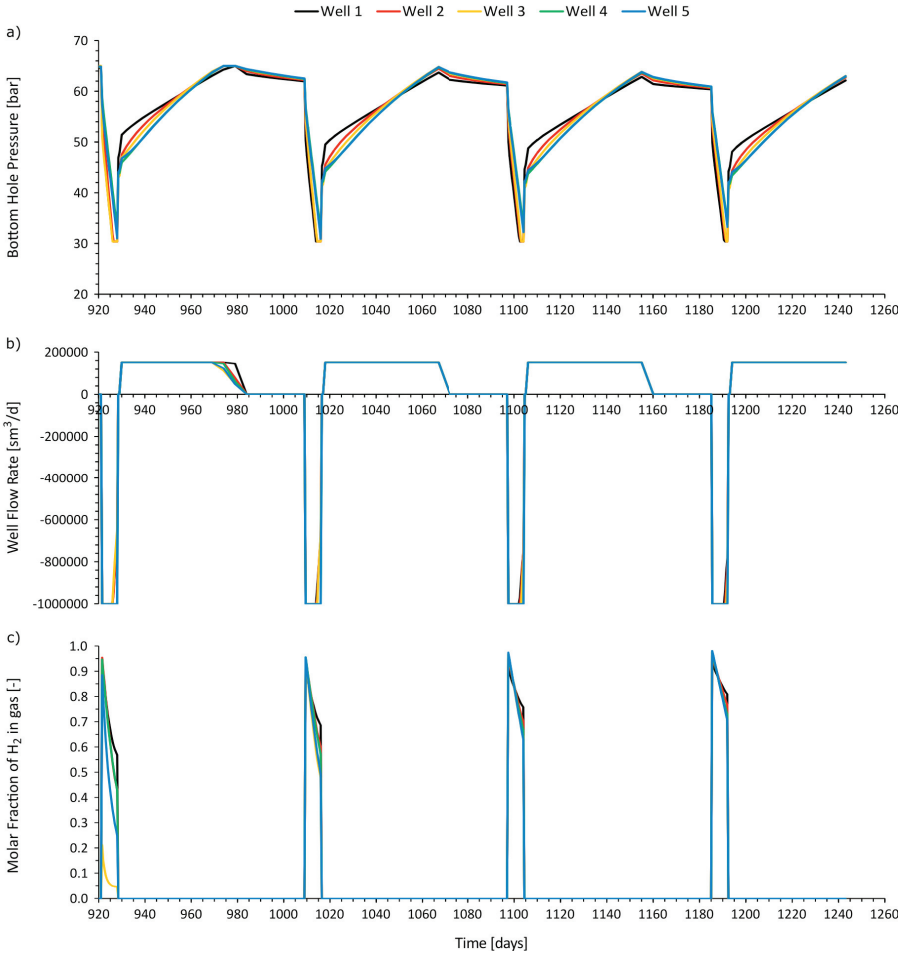

Fig. 4. (a) Bottom hole pressure; (b) gas flow rate; (c) H_2 in produced gas during the storage cycles.

components (Fig. 3c). The distribution of the hydrogen in the gas phase is mainly limited to the near vicinity of the injection wells, showing a more or less concentric spreading pattern. The propagation of hydrogen towards the north is somewhat damped compared to the initial filling with nitrogen. Different to the gas saturation, the composition of the gas phase clearly shows the current state of the storage operation.

The evolution of the bottom hole pressure during the third storage phase is similar for all wells (Fig. 4a). Immediately after the start of the extraction the bottom hole pressures decrease rapidly. During the extraction period wells 1, 2 and 3 quickly reach the lower pressure limit of 30 bar. Contrary to this, wells 4 and 5 only reach the lower pressure limit near the end of the extraction period. During the one day shut-in period which follows each extraction cycle, the bottom hole pressures quickly rebound to levels roughly representing the initial hydrostatic pressure. In the subsequent injection period, during which the storage is replenished with H_2, the bottom hole pressures increase again ultimately reaching the upper pressure limit at the end of the injection period. In the following 30 day shut-in period the pressures decline only slowly. As result the pressure signals are still at elevated levels at the beginning of the next extraction period. The general behavior of the pressures signals in the following storage cycles is comparable to that in the first cycle. However, the amplitudes of the pressure change are slightly smaller than in the first cycle.

The achieved gas flow rate at the wells is directly affected by the previously discussed bottom hole pressure as the applied injection or extraction rates are reduced when the upper or lower pressure limits are reached. Since the lower pressure limit is reached in most of the wells during the extraction periods, the achieved gas flow rates also differ from

Table 2. Volumetric results of the simulated storage.

Property	1^{st} cycle	2^{nd} cycle	3^{rd} cycle	4^{th} cycle
Av. gas extraction rate [sm^3/day]	4537663.45	4847096.32	4898459.86	4937376.33
Av. H_2 fraction in produced gas [%]	52.00	74.00	81.00	85.00
Fraction of weekly energy consumption [%]	13.21	19.52	21.60	22.88
Deviation from target energy amount [%]	-51.00	-28.00	-20.00	-16.00
Produced water volume [sm^3]	12784.25	9237.75	7420.50	6137.17

the target rates at the end of each production cycle (Fig. 4b). It can also be observed that the upper pressure limit is reached at the end of the first injection period. In the subsequent injection periods the upper pressure limit is not reached in any of the wells.

Since the gas in the storage consists of two components, the composition of the produced gas phase must be taken into account when assessing the storage performance. In an ideal case of storage, the produced gas phase consists of pure H_2. The simulation however shows that the composition of the produced gas phase is a mixture of H_2 and N_2 and changes over time (Fig. 4c). Especially in the first production period the composition changes strongly. While the fraction of H_2 in gas drops down to around 55 % in the best performing well 1, a H_2 fraction of just 5 % is achieved at the end of the production period in the worst performing well 3. This low performance is a result of to the well being shut during the second phase of the storage operation, which resulted in a smaller amount of hydrogen being available for extraction initially. Over the course of the subsequent storage cycles the average fraction of hydrogen in the produced gas increases for all wells. Different to the first cycle, the center well 3 is on par with the other storage wells from the second cycle onwards. The increase in storage performance is a result of the slightly larger injection volume of hydrogen compared to the extracted gas volume in each cycle and the overall increasing share of hydrogen in the gas storage over time.

The key factors for storage performance are the achieved gas extraction rate, the fraction of H_2 in the produced gas phase and the produced water fraction. The volumetric data shows that the average gas extraction rate per well of the storage increases from around 4.5 mio. sm^3/day in the first storage cycle to over 4.9 mio. sm^3/day in the fourth storage cycle (Tab. 2). The volume-weighted average of the fraction of H_2 in the produced gas also increases from 52 % in the first to 85 % in the last cycle. The simulated storage thus has the capacity to supply 22.88 % of the total energy demand in the fourth storage cycle. The amount of produced water decreases from about 13000 sm^3 in the first storage cycle to just over 6000 sm^3 in the fourth cycle. Compared with the volume of gas which is extracted in the same period of time, the fraction of water is 0.04 % in the first and 0.02 % in the last cycle respectively. It can be expected that the storage performance will increase further, ultimately reaching the target of supplying around a quarter of the total energy demand stated in the scenario definition.

5. Conclusion

In this work, a basic scenario for porous media hydrogen storage was developed and the associated processes were simulated numerically using a realistic setting in Northern Germany. The investigated scenario resembles a case in which a week-long gap in energy production must be mitigated using energy storage. The results of the simulation indicate that porous media hydrogen storage is indeed a viable option to store large quantities of energy needed in such a scenario. In the final storage cycle, the simulated storage is capable of delivering slightly more than 20 % of the total energy demand stated in the scenario definition. It must also be noted, that the storage performance increases from the first to the fourth storage cycle, indicating that the initial setup of the storage is not ideal. Employing an optimized injection scheme including shut-in periods during the initial filling of the reservoir in order to decrease the pressure levels and thus improving well injectivity could increase the storage performance further. In order to better understand the feasibility of porous media hydrogen storage, several issues have to be addressed in future work. Among those are the resistance of the cap rocks to hydrogen penetration, the importance of gas diffusion for mixing of the gas components within the gas phase as well as biogeochemical interactions between the gas phase, residual water or brine and the rock matrix.

Acknowledgements

We gratefully acknowledge the funding of the ANGUS+ joint project by the German Federal Ministry of Education and Research (BMBF) as part of the Energy Storage Funding Initiative, grant number 03EK3022, as well as the support of the Project Management Jülich (PTJ).

References

[1] Carden PO, Paterson L. Physical, chemical and energy aspects of underground hydrogen storage. Int J Hydrogen Energy 1979;4:559-569.
[2] Foh S, Novlin M, Rockar E, Randolph P. Underground Hydrogen Storage. Report BNL 57275. Institute of Gas Technology; Chicago, USA.; 1979.
[3] Korpas M, Greiner CJ. Opportunities for hydrogen production in connection with wind power in weak grids. Renewable Energy 2008;33:1199-1208.
[4] Klaus T, Vollmer C, Werner K, Lehmann H, Müschen K. Energieziel 2050: 100% Strom aus erneuerbaren Quellen. Federal Environment Agency Germany; 2010.
[5] Gregory DP, Pangborn JB. Hydrogen energy. Annu Rev Energy 1976;1:279-310.
[6] Ogden JM. Prospects for building a hydrogen energy infrastructure. Annu Rev Energy Environ 1999;24:227-279.
[7] Carr S, Premier GC, Guwy AJ, Dinsdale RM, Maddy J. Hydrogen storage and demand to increase wind power onto electrical distribution networks. Int J Hydrogen Energy 2014;39:10195-10207.
[8] Crotogino F, Donadei S, Bünger U, Landinger H. Large-scale hydrogen underground storage for securing future energy supplies. In: Stolten D, Grube T, editors. Proceedings of the 18th WHEC; 2010 May16-221, Essen; Schriften des Forschungszentrums Jülich 78-4.
[9] Ministerium für Energiewende, Landwirtschaft, Umwelt und ländliche Räume des Landes Schleswig-Holstein, editor. Energiebilanz Schleswig-Holstein 2011. Kiel, Germany; 2013.
[10] Büchi FN, Hofer M, Peter C, Cabalzar UD, Bernard J, Hannesen U, Schmidt TJ, Closset A, Dietrich P. Towards re-electrification of hydrogen obtained from the power-to-gas process by highly efficient H_2/O_2 polymer electrolyte fuel cells. RSC Adv 2014;4:56319-56146.
[11] Kroniger D, Madlener R. Hydrogen storage for wind parks: A real options evaluation for an optimal investment in more flexibility. Applied Energy 2014;136:931-946.
[12] Edwards PP, Kuznetsov VL, David WIF, Brandon NP. Hydrogen and fuel cells: Towards a sustainable energy future. Energy Policy 2008;36:4356-4362.
[13] Forsberg CW. Sustainability by combining nuclear, fossil, and renewable energy sources. Progress in Nuclear Energy 2009;51:192-200.
[14] Gao D, Jiang D, Liu P, Li Z, Hu S, Xu H. An integrated energy storage system based on hydrogen storage: Process configuration and case studies with wind power. Energy 2014;66:332-341.
[15] Bennion DB, Thomas FB, Ma T, Imer D. Detailed protocol for the screening and selection of gas storage reservoirs. SPE 59738; SPE/CERI Gas Technology Symposium Calgary, Canada; 2010.
[16] Paterson L. The implications of fingering in underground hydrogen storage. Int J Hydrogen Energy 1983;8(1):53-59.
[17] Wang X, Economides M. Advanced natural gas engineering. Houston, Texas: Gulf Publishing Company; 2009.
[18] Baldschuhn R, Binot F, Fleig S, Kockel F. Geotektonischer Atlas von Nordwest-Deutschland und dem deutschen Nordsee-Sektor. Geologisches Jahrbuch A153; Hannover, Germany; 2001.
[19] Hese F. 3D Modellierung und Visualisierung von Untergrundstrukturen für die Nutzung des unterirdischen Raumes in Schleswig-Holstein [PhD thesis]. Kiel: University of Kiel; 2012.
[20] Fahrion H, Betz D. Geologischer Rahmen, Fund- und Fördergeschichte. In: Achilles H, Ahrendt H, editors. Das Gasfeld Thönse in Niedersachsen, ein Unikat. Stuttgart, Germany: Schweizerbart Science Publishers; 1991.
[21] Gaupp R. Zur Fazies und Diagenese des Mittelrhät-Hauptsandsteins im Gasfeld Thönse. In: Achilles H, Ahrendt H, editors. Das Gasfeld Thönse in Niedersachsen, ein Unikat. Stuttgart, Germany: Schweizerbart Science Publishers; 1991.
[22] Doornenbal JC, Stevenson AG, editors. Petroleum geological atlas of the southern permian basin area. EAGE Publications b. v. Houten; 2010.
[23] Jaritz W. Zur Entstehung der Salzstrukturen Nordwestdeutschlands. Geologisches Jahrbuch A10; Hannover, Germany; 1973.
[24] Brooks RH, Corey AT. Hydraulic properties of porous media. Hydrology Papers Colorado State University; Fort Collins, Colorado; 1964.
[25] Burton M, Kumar N, Bryant SL. CO_2 injectivity into brine aquifers: why relative permeability matters as much as absolute permeability. Energy Procedia 2009;1:3091-3098.
[26] Hildenbrand A, Schlömer S, Krooss BM. Gas breakthrough experiments of fine-grained sedimentary rocks. Geofluids 2002;2:3-23.
[27] Hildenbrand A, Schlömer S, Krooss BM, Littke R. Gas breakthrough experiments on pelitic rocks: Comparative study with N_2, CO_2 and CH_4. Geofluids 2004;4:61-81.
[28] Bachu S, Bennion B. Effects of in-situ conditions on relative permeability characteristics of CO_2-brine systems. Environ Geol 2008; 54:1707-1722.
[29] Wollenweber J, Alles S, Busch A, Krooss BM, Stanjek H, Littke R. Experimental investigation of the CO_2 sealing efficiency of caprocks. Int J Greenhouse Gas Control 2010; 4:231-241.
[30] Schlumberger N.V. ECLIPSE v2014.2 - Technical Description; 2014.
[31] Oldenburg C. Carbon dioxide as cushion gas for natural gas storage. Energy & Fuels 2003;17:240-246.
[32] Oldenburg C, Pan L. Utilization of CO_2 as cushion gas for porous media compressed air energy storage. Greenhouse Gas Sci Technol 2013;3:1-12.